IOP Conf. Series: Materials Science and Engineering **306** (2018) 012081 doi:10.1088/1757-899X/306/1/012081

Performance Analysis of a Static Synchronous Compensator (STATCOM)

M M Kambey and J D Ticoh*

Electrical Engineering Education Department, Universitas Negeri Manado

*jdticoh@unima.ac.id

Abstract. Reactive power and voltage are some of the problems in electric power supply and A Gate Turn Off (GTO) Static Synchronous Compensator (STATCOM) is one of the type of FACTS with shunt which can supply variable reactive power and regulate the voltage of the bus where it is connected. This study only discuss about the performance characteristic of the three phase six-pulse STATCOM by analysing the current wave flowing through DC Capacitor which depend on switching current and capacitor voltage wave. Simulation methods used in this research is started with a mathematical analysis of the ac current, dc voltage and current equations that pass STATCOM from a literature. The result shows the presence of the capacitor voltage ripple also alters the ac current waveform, even though the errors to be not very significant and the constraint of the symmetry circuit is valid if the source voltages have no zero sequence components and the impedances in all the three phases are identical. There for to improve STATCOM performance it is necessary to use multi-pulse 12, 24, 36, 48 or more, and/or with a multilevel converter.

1. Introduction

Variables of complex electrical power system always changes. The indicator can be seen in the change of voltage, current, active power, reactive power or frequency in the power system. The amount of reactive power reserves in the power system is an indicator of testability of the voltage [1]. Recent development of power electronics introduces the use of FACTS devices in power systems. FACTS devices are capable of controlling the network condition in a very fast manner and this unique feature of FACTS devices can be exploited to improve the transient stability of a system [2-4]. Reactive power compensation is an important issue in electrical power systems and shunt FACTS devices play an important role in controlling the reactive power flow to the power network and hence the system voltage fluctuations and transient stability [5, 6]. Depending on the power rating of the STATCOM, different topologies are used for the power converter. High power STATCOM (several hundreds of Mvars) normally use GTO-based, square-wave voltage-sourced converters (VSC), while lower power STATCOM (tens of Mvars) use IGBT based (or IGCT-based) pulse-width modulation (PWM) VSC.

There were some technique are used to enhance the dynamic performance of the STATCOM [7, 10-16]. However, the analysis of the basic form of STATCOM with three-phase six-pulses is still very useful for understanding other models. In this paper the model of a GTO-based STATCOM on an electrical power transmission system [17-19]. There were some problems according with enhancing STATCOM performance, but because the limitation of the resources so the purpose of this study only

to analyzing the AC current waveform, current wave flowing through DC Capacitor (i_{dc}) which depend on switching current and voltage wave capacitor (v_{dc}).

2. Methods

The methods used in this research are literature study, started with a mathematical analysis of the voltage and current equations that pass through the three phase six-pulse STATCOM. It's begun first by construct GTO STATCOM mathematical equation with three phase six pulse to express the characteristic of AC current waveform, current wave flowing through DC Capacitor (i_{dc}) which depend on switching current and voltage wave capacitor (v_{dc}). There was three assumes is taken in paper study, first the capacitor size is infinite and therefore the DC side voltage is constant, the second the losses in the circuit are neglected and the third each switch is turned on only once in a cycle of supply voltage and conducts for 180^0 each.

The STATCOM consists of a voltage-sourced converter (VSC), a magnetic circuit (MC), a shunt coupling transformer, a shunt breaker, and a control and protection unit. In a VSC, a number of square wave voltages are generated at fundamental frequency by operating the controllable semiconductor switches once per cycle of the fundamental frequency. A solid-state voltage source inverter with several Gate Turn Off thyristor switch-based valves, a DC link capacitor, magnetic circuit, and a controller [13-16], the number of thyristors and the various configurations of the magnetic circuit depend on the desired quality of AC waveforms generated by the controller. The DC link capacitor is switched through the inverter circuit and the required reactive power is injected to the transmission circuit [15]. The basic building block circuit of a high power GTO based STATCOM with six pulse used in this paper shown in Fig. 1. The circuit consists of six switches, made up of six GTO thyristors with antiparallel diodes connected as a six pulse bridge.

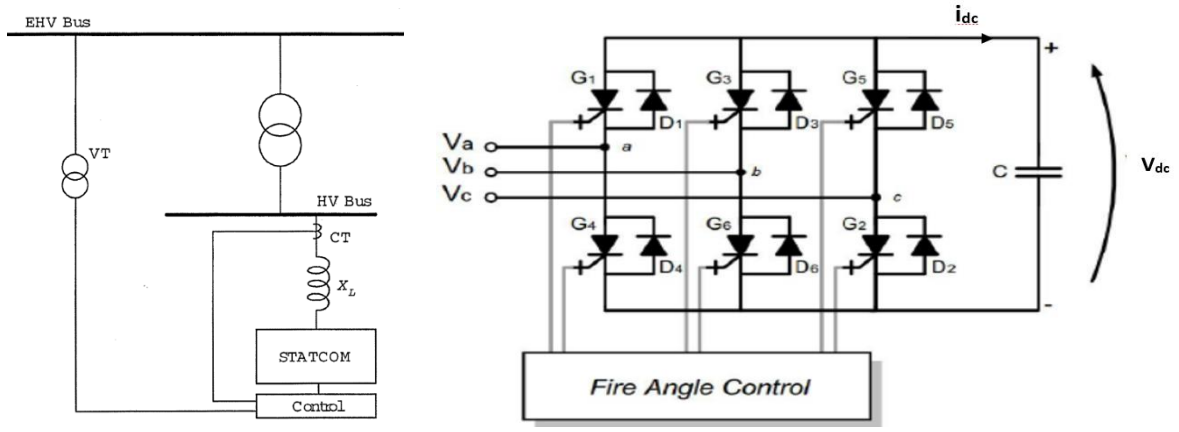

Figure 1. (a) STATCOM connection diagram. And (b) a three-phase six-pulse VSC circuit.

3. Results and Discussion

The waveform of the voltage (E_{aN}) as shown in Fig.2. The waveforms of E_{bN} and E_{cN} are also similar except that they are displaced from one another by 120^0. (E_{bN} lags E_{aN} by 120^0 dan (E_{cN} lags E_{bN} by 120^0) [19].

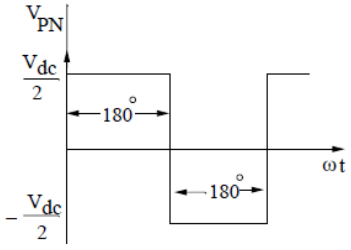

Figure 2. The waveform of V_{PN}.

The voltages E_{an}, E_{bn} dan E_{cn} respect to the source neutral can be obtained from the following equations

$$E_{an} = E_{aN} + V_{Nn} \quad (1)$$
$$E_{bn} = E_{bN} + V_{Nn} \quad (2)$$
$$E_{cn} = E_{cN} + V_{Nn} \quad (3)$$

Where the sum of the symmetry circuit $E_{an}, E_{bn}\ and\ E_{cn}$ is zero, and can be expressed as below

$$E_{an} + E_{bn} + E_{cn} = 0 \quad (4)$$

Substituting Eq. (4) in (1) to (3), we get

$$E_{Nn} = -\frac{E_{aN}+E_{bN}+E_{cN}}{3} \quad (5)$$

And

$$E_{aN} = \frac{2E_{aN}}{3} - \frac{E_{bN}}{3} - \frac{E_{cN}}{3}; \quad E_{bN} = \frac{2E_{bN}}{3} - \frac{E_{cN}}{3} - \frac{E_{aN}}{3}; \text{ and } E_{cN} = \frac{2E_{cN}}{3} - \frac{E_{aN}}{3} - \frac{E_{bN}}{3} \quad (6)$$

The waveform of E_{an} is shown in Fig. 3 (which also shows the supply Voltagev_a). The fundamental frequency component (rms value) of E_{an} is obtained as

$$E_{a1} = \frac{4}{\pi\sqrt{2}}\int_0^{\pi/2} E_{aN}\, sin\theta d\theta$$
$$= \frac{4}{\pi\sqrt{2}} V_{DC} = 0.45\, V_{dc} \quad (7)$$

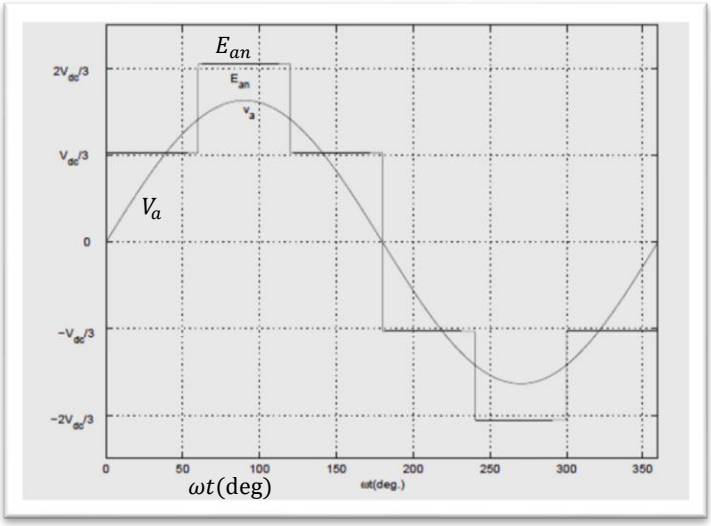

Figure 3. Waveforms E_{an} and v_a.

The harmonic component (E_{ah}) is obtained as

$$E_{ah} = \frac{E_{a1}}{h} = \frac{0.45V_{dc}}{h}, \qquad h = 6k \pm 1, \quad k = 1,2,3 \quad (8)$$

The rms value of the fundamental component of (reactive) current, I_r is calculated from

$$I_r = \frac{0.45V_{dc}}{\omega L} \quad (9)$$

The harmonic current (rms) is obtained as $I_h = \frac{0.45V_{dc}}{h^2\omega L}$ (10)

3.1 Analysis of AC current waveform

The instantaneous current in phase a (ia) is obtained from

$$L\frac{d_{ia}}{dt} = v_L(t) = v_a(t) - E_{an}(t) \quad (11)$$

Since $E_{aN}(t)$ varies depending on the interval in whichωt, lies, we get deferent expressions for $i_a(t)$ depending on the interval. However, in all intervals, $v_a(t) = \sqrt{2}\, V \sin \omega t$.

Interval 1, $0 \leq \omega t \leq 60^0$,

$$i_a(t) = \frac{V}{\omega L}\left[-\sqrt{2}\cos\omega t + \frac{V_{dc}}{V}\left(\frac{2\pi}{9} - \frac{\omega t}{3}\right)\right] \quad (12)$$

Interval 2, $60^0 \leq \omega t \leq 120^0$,

$$i_a(t) = \frac{V}{\omega L}\left[-\sqrt{2}\cos\omega t + \frac{V_{dc}}{V}\left(\frac{\pi}{3} - \frac{2\omega t}{3}\right)\right] \quad (13)$$

Interval 3, $120^0 \leq \omega t \leq 180^0$,

$$i_a(t) = \frac{V}{\omega L}\left[-\sqrt{2}\cos\omega t + \frac{V_{dc}}{V}\left(\frac{\pi}{9} - \frac{\omega t}{3}\right)\right] \quad (14)$$

The current in the interval, $180^0 \leq \omega t \leq 360^0$ is given by, $i_a(t) = i_a\left(t - \frac{\pi}{\omega}\right)$ (15)

Figure 4 shows the AC current waveforms (as calculated from Eqs (12) to (15) for V = 1:0, ωL=0,2, i_r=± 1,0. Both leading and lagging current waveforms are shown. As discussed earlier, the lagging current flows through the GTO thyristor switch 1 till $\omega t = 90^0$ and the reverse current flows through the antiparallel diode. Thus, the current °owing through the switch 1 is zero when it is turned off. On the other hand, switch 1 current starts from zero at $\omega t = 90^0$ when it is leading and is at a peak value when it is turned off. The peak GTO thyristor turn-off current (in the capacitive mode) is obtained from Eq. (17) (substituting $\omega t = 0^0$) expressed by

$$I_{Tpeak} = \frac{1}{\omega L}\left[\frac{2\pi V_{dc}}{9} - \sqrt{2V}\right] \quad (16)$$

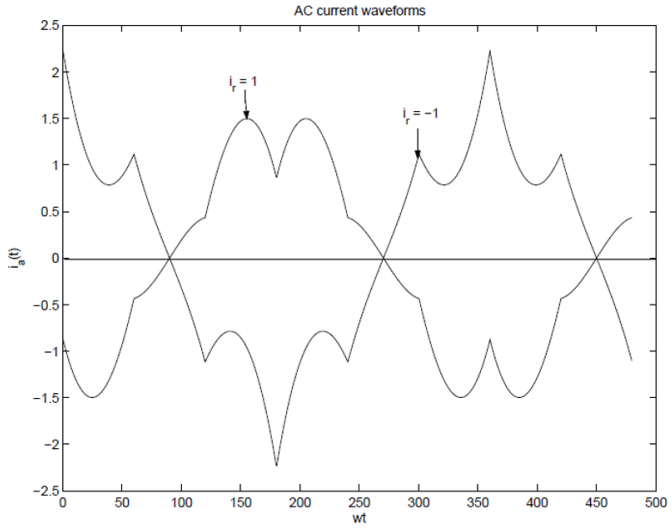

Figure 4. AC current Waveform.

3.2 Analysis of DC capacitor current and voltage

The current flowing through the DC capacitor (i_{dc}) is dependent on the switch currents. If we consider the interval, $0^0 < \omega t < 60^0$, the switches 5, 6 and 1 are conducting. In general, for any combination of switches, the following equation applies (neglecting losses in the switches).

$$V_{dc} i_{dc} = E_{an} i_a + E_{bn} i_b + E_{cn} i_c \quad (17)$$

The above is applicable at all times. Since E_{an}, E_{bn}, and E_{cn} are linearly dependent on V_{dc} (see Fig. 3), we can express them as

$$E_{an}(t) = S_a(t)V_{dc} + S_b(t)V_{dc} + S_c(t)V_{dc} \quad (18)$$

Where $S_a(t)$, $S_b(t)$ and $S_c(t)$ are termed as switching functions with constant values dependent on the interval considered. The switching functions are shown in Fig. 5. For the interval, $0 \leq \omega t < 60^0$, values of the switching functions are

$$S_a = \frac{1}{3}, S_b = -\frac{2}{3}, S_c = \frac{1}{3} \quad (19)$$

If we substitute Eq. (18) in (17), we get

$$i_{dc}(t) = S_a(t)i_a(t) + S_b(t)i_b(t) + S_c(t)i_c(t) \quad (20)$$

For the interval 1 ,$0 \leq \omega t < 60^0$, we get

$$i_{dc}(t) = \frac{1}{3}i_a(t) + -\frac{2}{3}i_b(t) + \frac{1}{3}i_c(t) \ = \frac{1}{3}[i_a(t) + i_b + \ i_c(t)] - i_b \qquad (21)$$

As the sum of phase currents,i_a, i_b and i_c s zero by Kirchcho's Current Law (KCL), we can simplify Eq. (21) as

$$i_{dc}(t) = \ -i_b(t) \ , 0 \leq \omega t < 60^0 \qquad (22)$$

It can be shown that (from symmetry)

$$-i_b(\omega t) = i_{a2}(\omega t + 60^0) \ = \frac{V}{\omega L}\left[\sqrt{2}sin(\omega t - 30^0) + \frac{V_{dc}}{V}\left(\frac{\pi}{2} - \frac{2\omega t}{3}\right)\right] \qquad (23)$$

Where $i_{a2}(\omega t)$ is the expression for $i_a(\omega t)$ in the interval, $60^0 \leq \omega t < 120^0$, given in Eq. (15). The capacitor current waveform in a cycle is obtained as the repetition of the waveform (from $0 \leq \omega t < 60^0$) over the remaining 5 intervals. It can be shown that the average value of the capacitor current is zero in steady state. (Otherwise the capacitor voltage cannot remain a constant). The fundamental component of this periodic waveform has the frequency of 6ω.

The capacitor voltage (v_c) was assumed as constant in the above analysis (due to infinite capacitance). However, with infinite capacitance, the capacitor voltage will have ripples. Assuming that the capacitor current $i_{dc}(t)$ is not affected by the voltage ripple, v_c can be obtained from

$$v_c(t) = V_0 + \frac{1}{C}\int i_{dc}(t)dt \qquad (24)$$

Where V_0 is the value of$V_{dc}(t)$ at t=0. Substituting Eq. (23) in (24), we get (for $0 \leq \omega t < 60^0$)

$$v_c(t) = V_0 - \frac{\sqrt{2}cos(\omega t - 30^0)}{\omega^2 LC} + \frac{V_{dc}\pi t}{9\omega LC} \ - \frac{2V_{dc}t^2}{6LC} + \frac{\sqrt{6}V}{2\omega^2 LC} \qquad (25)$$

The average value of $v_c(t)$ is $V_{dc}(t)$. This enables the calculation of V_0 as

$$V_0 = V_{dc}(t) - 0{,}061\frac{V_{dc}}{\omega^2 LC} + \frac{0{,}126V}{\omega^2 LC} \qquad (26)$$

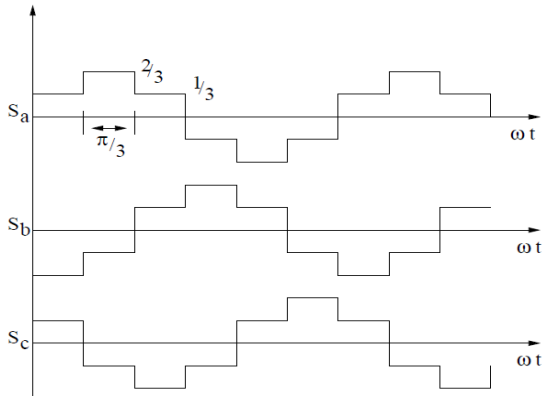

Figure 5. Switching functions.

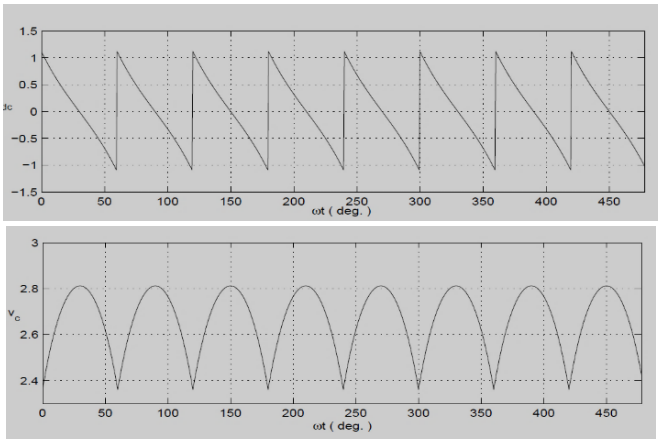

(a)

(b)

Figure 6. Waveforms of (a) i_{dc} and (b) v_{dc} for six pulse STATCOM.

The waveform of $v_c(t)$ for the interval, $0 \leq \omega t \leq 60^0$ is obtained after substituting Eq. (26) in (25). The waveform of $v_c(t)$ over the entire cycle is a repetition of the waveform for the interval $0 \leq \omega t \leq 60^0$. The waveforms of $i_{dc}(t)$ dan $v_c(t)$ over a complete cycle are shown in Fig.6 above. For V=1,0 pu, i_r= -1,0, ωL=0,2 and ωC=0,6.

And to determine the GTO thyristors and diodes rating voltages it is necessary to calculate the peak value of the capacitor voltage (V_{pk}), by substituting $\omega t = 30^0$ in the expression given by Eq. (25). We get,

$$V_{pk} = V_{dc} + \frac{0,03V_{dc}}{\omega^2 LC} + \frac{0,06V}{\omega^2 LC} \qquad (27)$$

4. Conclusions

The presence of the capacitor voltage ripple also alters the AC current waveform. However, the errors in the expressions of the instantaneous ac current waveform in phase a, i_a, on the interval 1, 2 and 3 can be assumed to be not very significant. As the capacitor voltage (v_c) was assumed as constant in the above analysis (due to infinite capacitance). However, with infinite capacitance, the capacitor voltage will have ripples. Assuming that the capacitor current idc (t) is not affected by the voltage ripple. The objective in deriving these analytical expressions is to gain insight. Such approximate analysis is quite common in power electronics as the first step towards a detailed analysis based on more exact models. There for to improve STATCOM performance it is necessary to use multi-pulse 12, 24, 36, 48 or more, and/or with a multilevel converter.

References

[1] Weedy B M, Cory B J, Jenkins N, Ekanayake J B and Strbac G 2012 *Electric power systems* (John Wiley & Sons).
[2] Flourentzou N, Agelidis V G and Demetriades G D 2009 VSC-based HVDC power transmission systems: An overview *IEEE Transactions on power electronics* **24**(3) pp. 592-602.
[3] Rashid M H 2009 *Power electronics: circuits, devices, and applications* (Pearson Education India).
[4] Murali D, Rajaram M and Reka N 2010 Comparison of FACTS devices for power system stability enhancement *International Journal of Computer Applications* **8**(4) pp. 30-5.
[5] Dixon J, Moran L, Rodriguez J and Domke R 2005 Reactive power compensation technologies: State-of-the-art review *Proceedings of the IEEE* **93**(12) pp. 2144-64.
[6] Panda S and Patel R N 2006 Improving power system transient stability with an off-centre location of shunt FACTS devices *Journal Of Electrical Engineering-Bratislava* **57**(6) pp. 365.
[7] Norouzi A H and Sharaf A M 2005 Two control schemes to enhance the dynamic performance of the STATCOM and SSSC *IEEE Transactions on Power delivery* **20**(1) pp. 435-42.
[8] Mienski R, Pawelek R and Wasiak I 2004 Shunt compensation for power quality improvement using a STATCOM controller: modelling and simulation *IEE Proceedings-Generation, Transmission and Distribution* **151**(2) pp. 274-80.
[9] El-Moursi M S and Sharaf A M 2005 Novel controllers for the 48-pulse VSC STATCOM and SSSC for voltage regulation and reactive power compensation *IEEE Transactions on Power systems* **20**(4) pp. 1985-97.
[10] Townsend C D, Summers T J, Vodden J, Watson A J, Betz R E and Clare J C 2013 Optimization of switching losses and capacitor voltage ripple using model predictive control of a cascaded H-bridge multilevel StatCom *IEEE Transactions on Power Electronics* **28**(7) pp. 3077-87.
[11] W Pan, Z Xu and J Zhang 2007 Novel configuration of 60-pulse voltage source converter for STATCOM application *International Journal of Emerging Electric Power Systems* **8**(5).
[12] M S El-Moursi and A M Sharaf 2005 Novel Controllers for the 48-Pulse VSC STATCOM and SSSC for Voltage Regulation and Reactive Power Compensation *IEEE Transactions on Power Systems* **20**(4) pp 1985-1997.

[13] Sen K 1999 STATCOM-STATic synchronous COMpensator: theory, modeling, and applications. In Power Engineering Society 1999 *Winter Meeting* IEEE 1999 Feb (Vol. 2, pp. 1177-1183). IEEE.
[10] Rashid M H 2010 *Power electronics handbook: devices, circuits and applications* (Academic press).
[14] Arvind P and Nitin S 2013 Transient Stability Improvement by Using Shunt FACTS Devices (STATCOM) with Reference Voltage Compensation (RVC) Control Scheme *International Journal of Electrical, Electronics and Computer Engineering, IJEECE* **2**(1) pp 7-12.
[15] Peng F Z, Qian W and Cao D 2010 *Recent advances in multilevel converter/inverter topologies and applications*. In Power Electronics Conference (IPEC) 2010 International 2010 Jun 21 (pp. 492-501). IEEE.
[16] Dávalos R, Ramirez J M and Tapia R 2005 Three-phase multi-pulse converter StatCom analysis *International Journal of Electrical Power & Energy Systems* **27**(1) pp. 39-51.
[17] Chakrabartis R, Chakraborty S, Mitra S, Choudhury R R, Chowdhury, Mondal S S and Halder S SVC Operation in Electric Transmission Line *International Journal of Emerging Technology and Advanced Engineering* **5**(8).
[18] Kowsalya M, Ray K K and Kothari D P 2009 Positioning of SVC and STATCOM in a Long Transmission Line *International Journal of Recent Trends in Engineering* **2**(5) pp. 150-154.
[19] Padiyar K R *FACTS controllers in power transmission and distribution*.